Simulating gravitational wave based measurements of the Hubble constant

Rachel Stromswold, Elizabeth Champion, Junjie Wang, Zhigong Gao
Department of Physics and Astronomy, University of Rochester
(Dated: May 7, 2022)

In this paper we consider a method for estimating the Hubble constant based on "dark sirens", gravitational wave observations which do not have a known electromagnetic counterpart. This method has already been applied to the event GW170814, but more observations are needed to constrain H_0 sufficiently to resolve the discrepancy between estimates produced by the Planck collaboration using high-redshift measurements of the cosmic microwave background and those produced by Riess et al. using low-redshift measurements of type Ia Supernovae. Using simulated events based on existing gravitational wave detections, we are able to estimate that $53 + 4 - 2$ observations of black hole mergers are needed to measure H_0 to an uncertainty of 5 $\mathrm{km\,s^{-1}\,Mpc^{-1}}$.

Keywords: Hubble's constant, gravitational wave, dark siren

I. INTRODUCTION

Hubble's law, the observation that galaxies are moving away from the Earth at a velocity proportional to their distance from the Earth, has been widely accepted since it was first proposed in the 1920s [1]. The constant of proportionality in this relationship is known as the Hubble parameter H. The Hubble parameter in general changes with time, and therefore with redshift z. By convention, the Hubble parameter at the current time ($t = 0$) is labeled H_0. For objects relatively close to the Earth (i.e. those at low redshift), the redshift is linearly related to the distance d by [2]

$$cz = H_0 d. \tag{1}$$

Here, c is the speed of light in a vacuum.

Variations in the physical assumptions underlying calculations of the Hubble constant, namely those used to compute the distances to objects at particular redshifts, have resulted in differing Hubble constant estimations. Hubble's initial estimation, determined by a simple linear fit between recession velocity and distance, gave roughly 500 $\mathrm{km\,s^{-1}\,Mpc^{-1}}$ [1]. Subsequent measurements have progressively refined this estimate, eventually stabilizing at approximately 70 $\mathrm{km\,s^{-1}\,Mpc^{-1}}$ [2]. However, different measurement approaches have led to significant disagreement between estimates: measurement uncertainties continue to diminish as methods improve, but the range of measured values does not. Figure 1 gives an overview of recent measurements showing significant disagreement.

There are two dominant methods for estimating the Hubble constant which are in tension with one another. The first uses low redshift measurements of standard candles, e.g. type Ia Supernovae, in order to determine H_0. The current estimate using this method is $H_0 = 74.03 \pm 1.42\ \mathrm{km\,s^{-1}\,Mpc^{-1}}$ [15]. Another approach, utilizing high redshift measurements of the cosmic microwave background (CMB), gives a value of $H_0 = 67.36 \pm 0.56$ $\mathrm{km\,s^{-1}\,Mpc^{-1}}$ [4].

It is highly unlikely that the discrepancy between these measurements, at greater than 4σ, can be explained as a statistical fluctuation or as the result of systematic uncertainties. For instance, Tamara et al. states that even small systematic errors in redshift will have a significant impact on measurements of H_0; however, this is not enough to account for the tension in H_0 [19]. See e.g. Efstathiou et al. and Calabrese et al. [20, 21] for further discussion of systematic uncertainties.

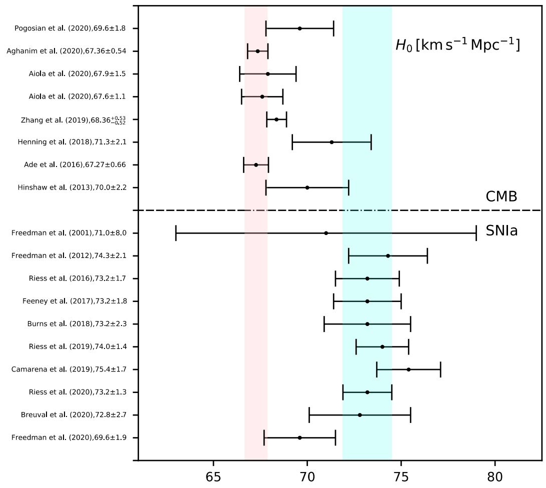

Figure 1. A selection of recent H_0 measurements demonstrating the significant discrepancies in its value [3–18]. Note that measurements are separated according to measurement type (i.e. CMB or SNIa).

A method for determining H_0 that does not rely on standard candles could potentially help resolve the tension in measurements of the Hubble constant. In this paper we consider an approach utilizing gravitational waves as an independent distance measurement.

II. METHODS

Binary black hole mergers are often called "dark sirens" due to their lack observable electromagnetic (EM) counterparts. Though the detection of an EM counterpart can facilitate the determination of the host galaxy and therefore result in a well-constrained measurement of H_0 [22], such detections are rare: at time of writing, GW170817 is the only neutron star merger detection with an identified EM counterpart [23].

As early as 1986 it was proposed that an array of multiple gravitational wave detectors could be used to estimate the distance to an event d_L and bounds on sky location [24]. Gravitational waves originating from a binary black hole system during the inspiral phase of the merger can be used as dark sirens due to the fact that the individual black hole masses can be determined from the gravitational wave frequency. The power radiating from the binary system is due to its orbital energy, and therefore the power radiating from the source can be determined purely from the gravitational wave frequency without any knowledge of the luminosity distance. The power detected is related to this emitted power through an inverse square law, and so the luminosity distance can be determined without the need for a cosmic distance ladder. Gravitational waves therefore present a completely independent method by which we can determine distances to galaxies, provided we can determine the host galaxy for a given merger [22, 25, 26].

Since we can estimate the sky location from which the signal was emitted along with the distance to the event, these estimates can then be used to produce a catalog of candidate host galaxies from existing sky surveys. Based on the posterior distributions for these localizations, we use a method for measuring H_0 laid out by Nair et al. [26]. It has been predicted that these methods can confine the Hubble constant within the decade [27]. This technique was applied to the event GW170814 by collaborators from the LIGO and Virgo teams using results from the Dark Energy Survey of the southern sky [25]. We carry out a similar analysis on simulated data sets based on historic gravitational wave (GW) data and simple physical assumptions for the distribution of galaxies within clusters. To show the validity of our analysis, we generate our simulated data sets using a specific value of H_0 and confirm that we can recover this value.

Historic data is taken from merger catalogs from the second and third year of LIGO observations [28, 29]. Our analysis is only interested in the solid angle covered by sky localization (Ω), distances obtained from the GW data (d_L), and their uncertainties, σ_d. We thus marginalize over all other parameters to obtain a three dimensional probability distribution containing only these parameters of interest. It vastly simplifies our analysis if we assume that the uncertainties on d_L are Gaussian. However, posterior distributions from the LIGO papers contain differing upper and lower credible limits. To compensate, we take the half width on these posteriors as our Gaussian uncertainties.

After obtaining these marginalized probability distributions, we use historic data as a training set for Gaussian kernel density estimation. We then use the kernel estimation to sample simulated events which have the same underlying probability distribution as observations. The returned samples have a finite probability to be from unphysical regions, i.e. $d_L \leq 0$, $\Omega \leq 0$ or $\sigma_d > d_L$. To counteract this, we reject all samples that are outside of the extremal historic values (e.g. if a sample is closer than the closest observed detection we reject it), or that violate the $\sigma_d \leq d_L$ constraint. Many of the sampled events will have very large localization regions, which makes it inconvenient to use them for estimates of H_0. Since our goal is to produce an estimate of how many observations are required to produce estimates of H_0 we only perform further analysis on events that were well localized.

In principle, one should consider the posterior distribution on sky location which has a finite probability to be found outside the credible interval. To simplify our analysis, we approximate this probability distribution as uniform within the localization volume and zero everywhere else. This treatment has precedent in existing studies [25, 26].

After producing simulated GW events and their corresponding localization volumes, we need to select a suitable sky catalog. These data are also simulated by randomly sampling a number of galaxy clusters which are assumed not to interact with one another. The total mass of the cluster is assumed to follow a Press-Schechter mass distribution [30]. Peculiar motions (which affect the measured redshift z) and distance from the center of mass are sampled such that the virial theorem is obeyed, but other important factors like the very high concentrations of dark matter within clusters are neglected. More details on cluster generation are given in Appendix A.

We start with a simple application of Bayes' theorem,

$$\begin{aligned} p(H_0|d_{GW}, d_C) &\propto p(d_{GW}, d_C|H_0)p(H_0) \\ &= p(d_{GW}|H_0)p(d_C|H_0)p(H_0), \end{aligned} \quad (2)$$

where d_{GW} refers to the observed data from the gravitational wave detectors and d_C refers to data from the known catalog of stars and their redshifts. We break this joint likelihood into a product of likelihoods since both experiments are statistically independent.

Since we are considering dark sirens without EM counterparts, we do not know the host galaxy in which the merger occurred. Thus we must marginalize over all galaxies within the volume of possible locations supplied by the GW data. Since the number of galaxies is discrete, this is expressed as a sum:

$$\begin{aligned} & p(d_{GW}, d_C|z_j, \hat{\Omega}_j, H_0) \propto \\ & \quad \sum_i w_i \int dV p(d_{GW}|d_L, \hat{\Omega}_{GW}) p(d_C|z, \hat{\Omega}_j) \\ & \quad \delta_D(d_L - d_L(z_i, H_0)) \delta_D(\hat{\Omega}_{GW} - \hat{\Omega}_i). \end{aligned} \quad (3)$$

In principle, we should apply a weight w_i to each galaxy, but for simplicity we take $w_i = 1$ for all galaxies within the volume of interest and $w_i = 0$ for all galaxies outside. This same approximation has been used in previous analyses [25–27]. To evaluate this integral we switch to spherical coordinates and work in redshift space as opposed to distance space. This results in a change of coordinates

$$dV \propto \frac{d^2V}{dz_i d\hat{\Omega}_i}\frac{dz_i}{dr}dr d\hat{\Omega} \propto \frac{r^2(z_i)}{H(z_i)} \tag{4}$$

where $H(z_i)$ is the Hubble parameter in redshift space,

$$H(z_i) = H_0^3\left(\Omega_m(1+z)^3 + \Omega_\Lambda\right), \tag{5}$$

where we have assumed a flat universe. We will take $\Omega_m = 0.3$ and $\Omega_\Lambda = 0.7$ in keeping with Soares-Santos et al [25]. We expect our catalog of galaxies to have very low uncertainty on sky location, so we take $p(d_C|z_i,\Omega) = p(d_C|z_i)\delta(\Omega - \Omega_i)$. Finally we can write the posterior distribution for H_0:

$$p(H_0|d_{GW}, d_C) \propto p(H_0)\sum_i \frac{1}{Z_i} \times \int dz_i p\left(d_{GW}|d_L(z_i,H_0),\hat{\Omega}_i\right) p(d_C|z_i)\frac{r^2(z_i)}{H(z_i)} \tag{6}$$

where $d_L(z_i, H_0) = cz_i/H_0$ uses Hubble's law to express luminosity distance in terms of redshift and an assumed value for H_0. In keeping with Singer et al., we assume that the errors on redshifts are Gaussian [31]. Under this assumption,

$$p\left(d_{GW}|d_L(z_i,H_0)\right) \propto \frac{p(\hat{\Omega})}{\sqrt{2\pi}\sigma(\hat{\Omega})}\exp\left(-\frac{(cz_i/H_0 - \hat{d}_{GW})^2}{2\sigma_{GW}^2}\right). \tag{7}$$

III. RESULTS

We produce simulated events until we find at least 100 with sufficiently small localizations that further analysis is practical. This cutoff is arbitrary. For all results reported, we used a maximum volume of 0.5×10^9 Mpc^3. We also observed values which had anomalously small localization volumes so we constrained all simulated events to have a localization volume larger than 0.5×10^7 Mpc^3. We found that a total of 650 observations were needed to produce the desired 100 well localized events. These localized regions corresponded to 15.43% of all generated samples. In all of our tests we injected a known value of $H_0 = 70$ km s^{-1} Mpc^{-1}. Quoted results and figures repeated this procedure 10 times and averaged over each instance.

The resulting posterior $p(H_0|d_{GW}, d_C)$ produced after 100 observations is shown in Figure 2 along with the posterior obtained from each observation considered in isolation. In Figure 3 we show the standard deviation of the posterior $p(H_0|d_{GW}, d_C)$ as a function of number of localized events. In Figure 4 we show the deviation of the posterior expectation on H_0 from the known value as a function of number of well localized events. We can see that our posterior produces an underestimate of H_0. This suggests that there are as yet unidentified systematic effects that need to be taken into account. Figure 5 shows a correlation between the means and standard deviations of the posterior distributions for single events. This correlation would clearly bias our estimate of H_0 towards lower values, since these have smaller standard deviations and thus higher constraining power. The origin of this correlation is therefore likely to be the unidentified systematic effect.

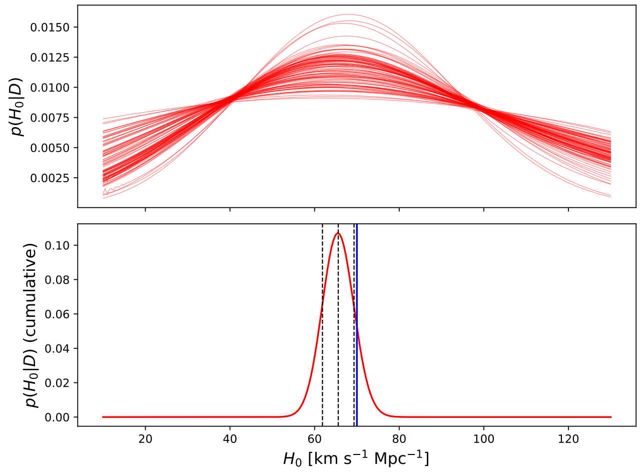

Figure 2. Upper: Posteriors produced from individual events. The bias of posteriors with poorer localization is noticable, and is probably contributing to the underestimate of H_0 that we note. Lower: The posterior $p(H_0|d_{GW}, d_C)$ produced after 100 samples. The 68% credible interval is shown by the dashed lines. The true injected value is shown in blue.

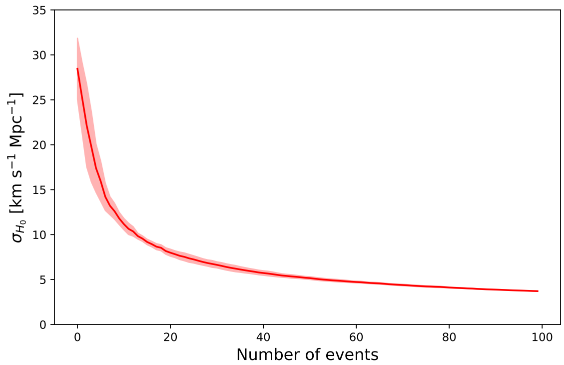

Figure 3. The standard deviation obtained from the posterior $p(H_0|d_{GW}, d_C)$. The shaded region shows uncertainty from the population average.

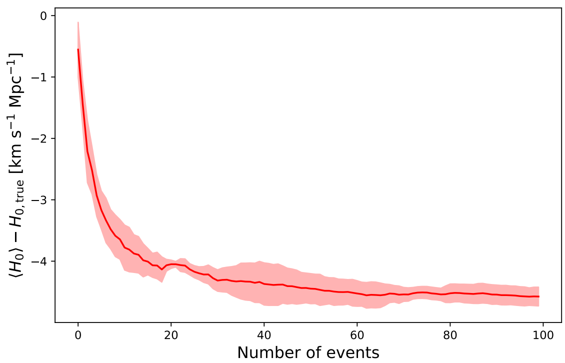

Figure 4. The deviation between the injected known value of H_0 and our expectation value based on $p(H_0|d_{GW}, d_C)$. The shaded region shows uncertainty from the population average.

IV. DISCUSSION

In this paper we have considered a measurement of the Hubble constant H_0 using the luminosity distances of binary black hole mergers estimated from their gravitational wave signals. By simulating the effects of future detections using a physically plausible (though simplified) model of galaxy clusters, we determine that the constraints resulting from such measurements can become considerably smaller. In particular, we find that after $53 + 4 - 2$ detections with sufficient sky localization, the standard deviation on the measurement of H_0 could reach roughly 5 $\mathrm{km\,s^{-1}\,Mpc^{-1}}$.

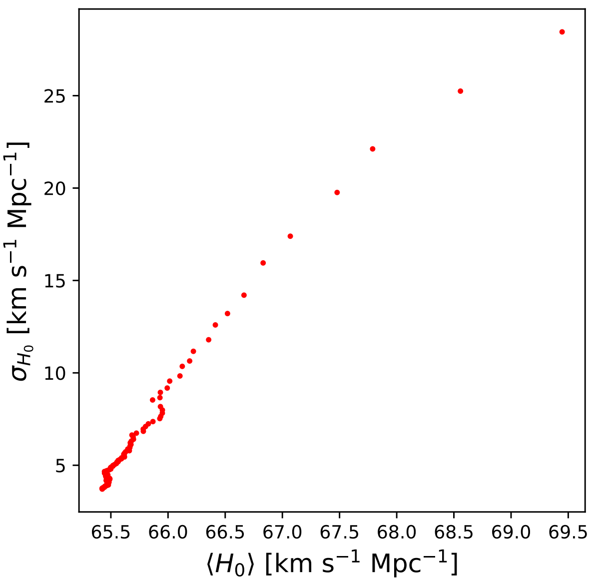

Figure 5. The means and standard deviations of the estimates on H_0 for individual events. Note the clear correlation between these quantities.

This measurement of H_0 is independent of the standard candles used in other calculations, and thus presents a possible means of confirming or rejecting these other calculations, which are in tension with one another. However, careful consideration must be given to systematic biases and uncertainties in this analysis. In particular we see a strong correlation between the measured value of H_0 for a particular event and the standard deviation associated with that measurement, as shown in Figure 5. The origin of this correlation is likely to be some systematic bias in the analysis, and future work should determine whether this bias would be present in real data or if it is a result of our simplified galaxy cluster model.

[1] E. Hubble, Proceedings of the National Academy of Sciences **15**, 168 (1929), https://www.pnas.org/doi/pdf/10.1073/pnas.15.3.168.

[2] W. L. Freedman and B. F. Madore, Annual Review of Astronomy and Astrophysics **48**, 673 (2010), https://doi.org/10.1146/annurev-astro-082708-101829.

[3] L. Pogosian, G.-B. Zhao, and K. Jedamzik, The Astrophysical Journal **904**, L17 (2020).

[4] Planck Collaboration, N. Aghanim, Y. Akrami, M. Ashdown, J. Aumont, *et al.*, Astronomy and Astrophysics **641** (2020).

[5] S. Aiola, E. Calabrese, L. Maurin, S. Naess, B. L. Schmitt, *et al.*, Journal of Cosmology and Astroparticle Physics **2020**, 047 (2020).

[6] X. Zhang and Q.-G. Huang, "Constraints on h_0 from wmap and baryon acoustic osillation measurements," (2018).

[7] J. W. Henning, J. T. Sayre, C. L. Reichardt, P. A. R. Ade, A. J. Anderson, *et al.*, The Astrophysical Journal **852**, 97 (2018).

[8] P. A. R. Ade, N. Aghanim, M. Arnaud, M. Ashdown, J. Aumont, *et al.*, Astronomy and Astrophysics **594**, A13 (2016).

[9] G. Hinshaw, D. Larson, E. Komatsu, D. N. Spergel, C. L. Bennett, *et al.*, The Astrophysical Journal Supplement Series **208**, 19 (2013).

[10] W. L. Freedman, B. F. Madore, B. K. Gibson, L. Ferrarese, D. D. Kelson, *et al.*, Astrophys. J. **553**, 47 (2001), arXiv:astro-ph/0012376 [astro-ph].

[11] W. L. Freedman, B. F. Madore, V. Scowcroft, C. Burns, A. Monson, *et al.*, Astrophys. J. **758**, 24 (2012), arXiv:1208.3281 [astro-ph.CO].

[12] A. G. Riess, L. M. Macri, S. L. Hoffmann, D. Scolnic, S. Casertano, *et al.*, Astrophys. J. **826**, 56 (2016), arXiv:1604.01424 [astro-ph.CO].

[13] S. M. Feeney, D. J. Mortlock, and N. Dalmasso, Monthly Notices of the Royal Astronomical Society **476**, 3861 (2018).

[14] C. R. Burns, E. Parent, M. M. Phillips, M. Stritzinger, K. Krisciunas, *et al.*, The Astrophysical Journal **869**, 56 (2018).

[15] A. G. Riess, S. Casertano, W. Yuan, L. M. Macri, D. Scolnic, *et al.*, The Astrophysical Journal **876**, 85 (2019).

[16] D. Camarena and V. Marra, Physical Review Research **2** (2020), 10.1103/physrevresearch.2.013028.

[17] A. G. Riess, S. Casertano, W. Yuan, J. B. Bowers, L. Macri, J. C. Zinn, and D. Scolnic, The Astrophysical Journal Letters **908**, L6 (2021).

[18] L. Breuval, P. Kervella, R. I. Anderson, A. G. Riess, F. Arenou, *et al.*, Astronomy and Astrophysics **643**, A115 (2020).

[19] T. M. Davis, S. R. Hinton, C. Howlett, and J. Calcino, Monthly Notices of the Royal Astronomical Society **490**, 2948 (2019).

[20] G. Efstathiou and S. Gratton, The Open Journal of Astrophysics **4** (2021), 10.21105/astro.1910.00483.

[21] E. Calabrese, A. Slosar, A. Melchiorri, G. F. Smoot, and O. Zahn, Physical Review D **77** (2008), 10.1103/physrevd.77.123531.

[22] B. P. Abbott, R. Abbott, T. D. Abbott, F. Acernese, K. Ackley, *et al.*, Nature **551**, 85 (2017).

[23] B. P. Abbott, R. Abbott, T. D. Abbott, F. Acernese, K. Ackley, *et al.* (LIGO Scientific Collaboration and Virgo Collaboration), Phys. Rev. Lett. **119**, 161101 (2017).

[24] B. Schutz, Nature (London) **323**, 310 (1986).

[25] M. Soares-Santos, A. Palmese, W. Hartley, J. Annis, J. Garcia-Bellido, *et al.*, The Astrophysical Journal **876**, L7 (2019).

[26] R. Nair, S. Bose, and T. D. Saini, Physical Review D **98**, 023502 (2018), arXiv: 1804.06085.

[27] H.-Y. Chen, M. Fishbach, and D. E. Holz, Nature (London) **562**, 545 (2018), arXiv:1712.06531 [astro-ph.CO].

[28] R. Abbott, T. Abbott, S. Abraham, F. Acernese, K. Ackley, *et al.*, Physical Review X **11**, 021053 (2021).

[29] T. L. S. Collaboration, the Virgo Collaboration, the KAGRA Collaboration, R. Abbott, T. D. Abbott, F. Acernese, *et al.*, arXiv:2111.03606 [astro-ph, physics:gr-qc] (2021), arXiv: 2111.03606.

[30] W. H. Press and P. Schechter, Astrophys. J. **187**, 425 (1974).

[31] L. P. Singer, H.-Y. Chen, D. E. Holz, W. M. Farr, L. R. Price, *et al.*, apjs **226**, 10 (2016), arXiv:1605.04242 [astro-ph.IM].

[32] S. M. Hansen, T. A. McKay, R. H. Wechsler, J. Annis, E. S. Sheldon, and A. Kimball, The Astrophysical Journal **633**, 122 (2005).

[33] D. Clowe, M. Bradač, A. H. Gonzalez, M. Markevitch, S. W. Randall, C. Jones, and D. Zaritsky, The Astrophysical Journal **648**, L109 (2006).

[34] F. Hoh, Journal of Modern Physics , 967 (2020).

Appendix A: Simulated galaxy catalogs

After producing a simulated event, we need to produce a catalog of galaxies within the credible interval of sky locations and radial distances obtained from the GW event sample. The volumes produced by typical events are very large, on the order of 1 Gpc^3. Volumes this large will exhibit large scale structures. To simplify our analysis we only consider clusters of galaxies and not larger structures such as superclusters or filaments.

To estimate the density of galaxy clusters we use a survey by S. Hansen et al. of a 395 deg^2 region of sky observed in the SDSS catalog [32]. This analysis found 12830 clusters with redshifts in the range $0.07 \leq z \leq 0.3$, for which this catalog is considered complete. Using a value of $H_0 = 70\ \mathrm{km\,s^{-1}\,Mpc^{-1}}$, we arrive at a very crude estimate of cluster density of $1.5 \times 10^{-4}\ \mathrm{Mpc^{-3}}$.

Assuming that the mass of normal matter in a cluster follows the Press-Schechter function [30] and that the number of galaxies is proportional to mass we can express the probability distribution that a cluster has n galaxies as

$$p(n|n_c, \alpha) \propto \left(\frac{n}{n_c}\right)^{\alpha} e^{n/n_c} \tag{A1}$$

where n_c and α are paramters that should be fitted to the data. Using the SDSS catalog we obtain estimates $\alpha = 7.695$ and $n_c = 3$. The authors also find that the characteristic radius for a galaxy cluster goes as $r_c \, \mathcal{N}_{gals}^{\beta}$ for $\beta = 0.56$ [32]. We take the offset of any galaxy from the center of mass to follows a three-dimensional Gaussian distribution with $\sigma_r = r_c$. Under the assumption that the virial theorem is obeyed and that velocities follow a normal distribution, we can derive an expression for σ_v in terms of r_c:

$$\langle U \rangle = \frac{4\pi G\mu}{\sqrt{2\pi r_c^2}} \int r e^{-r^2/2r_c^2} dr = \sqrt{8\pi m} r_c = 2\pi m \sigma_v^2 = \langle K \rangle$$
$$\implies \sigma_v^2 = \frac{G r_c}{\sqrt{\pi/2}} \frac{\mu}{m}. \tag{A2}$$

Here we have taken μ to be the reduced mass of the galaxy and the center of gravity of the cluster. It is well known that galaxy clusters tend to be dominated by dark matter [33, 34]. Therefore, in all of our numerical work we use the approximation $\mu/m = 1$.

This model for catalog generation makes a number of unrealistic assumptions. We have treated cluster densities as uniform within the range of interest, but we should expect this to have a redshift dependence. We have also ignored the role of dark matter which should constitute the majority of a cluster's mass. It may be interesting to account for these affects in future work, but the model presented here is sufficient for a toy model. However, this model does produce correlations between the peculiar motions of galaxies and their locations, which is a useful test of the robustness of our estimation of Hubble's constant.

Now that we have described the details of our cluster generation procedure, we need to address one more important detail in our cluster generation. In order to make our data realistic, there should be a true host galaxy. We expect this galaxy to be near the center of our volume credible interval. To account for this, we select a cluster at random to contain the host where the probability that any given cluster contains the host is proportional to the number of galaxies it contains. After selecting this cluster, we move it to the center of the GW localization region and apply a Gaussian displacement.

To get a crude estimate of the width of this Gaussian displacement, we start by considering a sphere which has an equivalent volume. Assuming that this volume represents a 95% confidence interval, the radius of this galaxy should be 2σ. Thus, we select a Gaussian width on the host cluster displacement,

$$\sigma = \frac{1}{2} \left(\frac{3}{4\pi} V \right)^{1/3}. \tag{A3}$$

Appendix B: Data and Code

The code for both galaxy cluster simulation and the calculation of the posterior distribution of H_0, as well as the data products for each of these, can be found at `https://github.com/rachel-stromswold/phys403_final_project`.